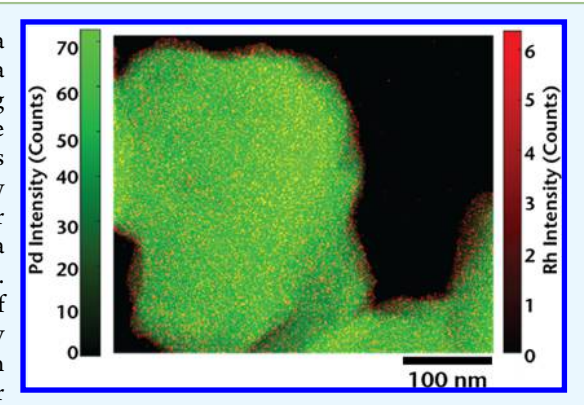


# **Enhanced Kinetics of Electrochemical Hydrogen Uptake and Release** by Palladium Powders Modified by Electrochemical Atomic Layer **Deposition**

David M. Benson, † Ochu F. Tsang, † Joshua D. Sugar, \* Kaushik Jagannathan, † David B. Robinson, \* Farid El Gabaly, Patrick J. Cappillino, And John L. Stickney,

ABSTRACT: Electrochemical atomic layer deposition (E-ALD) is a method for the formation of nanofilms of materials, one atomic layer at a time. It uses the galvanic exchange of a less noble metal, deposited using underpotential deposition (UPD), to produce an atomic layer of a more noble element by reduction of its ions. This process is referred to as surface limited redox replacement and can be repeated in a cycle to grow thicker deposits. It was previously performed on nanoparticles and planar substrates. In the present report, E-ALD is applied for coating a submicron-sized powder substrate, making use of a new flow cell design. E-ALD is used to coat a Pd powder substrate with different thicknesses of Rh by exchanging it for Cu UPD. Cyclic voltammetry and X-ray photoelectron spectroscopy indicate an increasing Rh coverage with increasing numbers of deposition cycles performed, in a manner consistent with the atomic layer deposition (ALD) mechanism. Cyclic



voltammetry also indicated increased kinetics of H sorption and desorption in and out of the Pd powder with Rh present, relative to unmodified Pd.

KEYWORDS: E-ALD, SLRR, palladium, rhodium, powder, electrodeposition, UPD, flow cell

# 1. INTRODUCTION

Atomic layer deposition (ALD) makes use of surface limited reactions in a cycle to form nanofilms conformally on a substrate. The result is material formation, one atomic layer at a time, where an atomic layer is not more than one atom in thickness. ALD is generally performed in a gas or vacuum phase reactor and has been remarkably successful in forming oxide nanofilms.2,

Electrochemical atomic layer deposition (E-ALD) is a condensed phase version of ALD, based on the use of underpotential deposition (UPD),<sup>4-6</sup> an electrochemical form of surface limited reaction. 7-9 UPD results from the favorable free energy of formation of a compound or an alloy and involves the deposition of one element on a second at a potential prior to ("under", generally meaning more positive than) that needed to deposit the element on itself. UPD generally results in the deposition of an atomic layer, with a maximum coverage of about one monolayer (ML), defined in this report as one adsorbate atom per substrate surface atom. E-ALD cycles consisting of surface limited redox replacement (SLRR) were used to deposit Rh. SLRR involves the deposition of an atomic layer of a sacrificial metal using UPD, which should be less noble than the metal to be deposited. 10-14 The

solution is then exchanged, at open circuit, for the one containing an ionic precursor for the desired element. The depositing element is reduced using electrons from the sacrificial UPD layer, the coverage of which accounts for limiting the amount of the desired element formed. Rinsing with a blank solution completes the SLRR cycle, which can be repeated to form thicker deposits. <sup>15–17</sup> E-ALD is used in the present study because of the control it offers over Rh nanofilm deposit coverages. SLRR on nanoparticles was previously demonstrated by Pt deposition on Au nanoparticles for oxygen reduction.18

Previous work has shown that modification of the surface of a Pd nanofilm with Rh<sup>19</sup> or Pt<sup>20,21</sup> using E-ALD resulted in enhanced rates for H absorption and desorption. This is expected because of a less stable surface hydride on Rh or Pt, as compared with Pd. Formation of a surface hydride is presumed to be an intermediate step to bulk absorption or desorption, and if the surface hydride is too stable, there will be a high

Received: March 1, 2017 Accepted: April 28, 2017 Published: April 28, 2017

<sup>&</sup>lt;sup>†</sup>Department of Chemistry, University of Georgia, Athens, Georgia 30602, United States

<sup>&</sup>lt;sup>‡</sup>Sandia National Laboratories, Livermore, California 94550, United States

<sup>§</sup>Department of Chemistry and Biochemistry, University of Massachusetts Dartmouth, North Dartmouth, Massachusetts 02747, United States

activation barrier to transport from the surface and a low concentration of vacant sites for transport to the surface.<sup>22,23</sup>

Studies of E-ALD have, thus far, primarily involved deposition on flat surfaces, 20,24-27 except for studies using SLRR, which was initially developed to coat the surfaces of nanoparticles with minimum quantities of catalytic metals. 11,28 The present study was undertaken to investigate similar deposits on the surfaces of three-dimensional materials in the form of submicron-sized powders. Such powders have applications in hydrogen separation, fuel cells, sensors, and catalysts. 29-32 Prior work on hydrogen reactions with powders has involved both elemental and alloy powders. 33-36 Powders typically allow for a much larger electrochemical surface area, for a given superficial surface area, compared with a planar substrate, increasing the rates of interfacial reactions. 7 Powders have been studied as media for storage or separation of bulk amounts of hydrogen. 38,39

Reports in the literature suggest that Pd powders with the surface modified by Rh or Pt enhance both hydrogen absorption and desorption. This report investigates the effect of Pd surface modification with SLRR Rh on the rates of hydrogen absorption and desorption, to find out whether the effect seen on films also applies to the more complex geometries and surface microstructures of powders. In the present study, hardware and methodologies for surface modification using E-ALD of Rh on large surface area powders were investigated. The use of E-ALD to modify powders will result in a much greater yield of the modified surface area than it would on planar substrates but requires certain considerations to ensure that the reactions can proceed uniformly and completely.

# 2. EXPERIMENTAL METHODS

All solutions were prepared using 18  $M\Omega$  cm water from a water filtration system (Milli-Q Advantage A10). The Rh solution contained 0.1 mM RhCl $_3$  (Sigma-Aldrich, 99.9%, trace metals basis) in 0.1 M  $H_2SO_4$  (Fisher, analytical grade). The sacrificial metal solution was 2 mM CuSO $_4$  (J.T. Baker, 99.8%) in 0.1 M  $H_2SO_4$ . The blank solution was 0.1 M  $H_2SO_4$ . During use and for at least 60 min prior, all solutions were degassed with  $N_2$  to remove dissolved  $O_2$ .

E-ALD experiments were performed using an automated flow cell system (Electrochemical ALD, L.C.) consisting of a variable speed pump, a solenoid selection valve, solution reservoirs, a potentiostat, and a three-electrode flow cell. Sequencer 4.0 control software (Electrochemical ALD, L.C.) was used to form the deposits. The flow cell (Figure 1) was designed to hold powdered substrates, and it allowed solution exchange while under potential control. The design consisted of two sides, each with flat silica frits. The sample was placed between the frits, inside of two pieces of a nitrocellulose filter paper (Millipore, 0.45  $\mu$ m). Two rubber gasket rings were placed around the substrate, which prevented leakage at the joint. Electrical contact was made using a piece of Teflon-coated Pt wire (Med Wire), where the stripped end was placed inside of the Pd powder substrate, and the Teflon-coated region passed between the two gaskets. The entire ensemble was held together with a metal clamp. A Pt mesh cage (diameter 0.5", length 2") served as the auxiliary electrode and was housed in the upper column. A reference electrode compartment, containing an Ag/AgCl (3 M KCl) electrode (Bioanalytical Systems, Inc.), was located at the ingress to the cell. All potentials were reported versus the Ag/AgCl reference electrode. The solutions were drawn from reservoirs through a valve block and then pumped past the reference electrode and through the powdered working electrode. After the working electrode, the solutions entered the auxiliary electrode compartment, from which they were pumped to waste along with any gaseous products produced at the auxiliary electrode. All

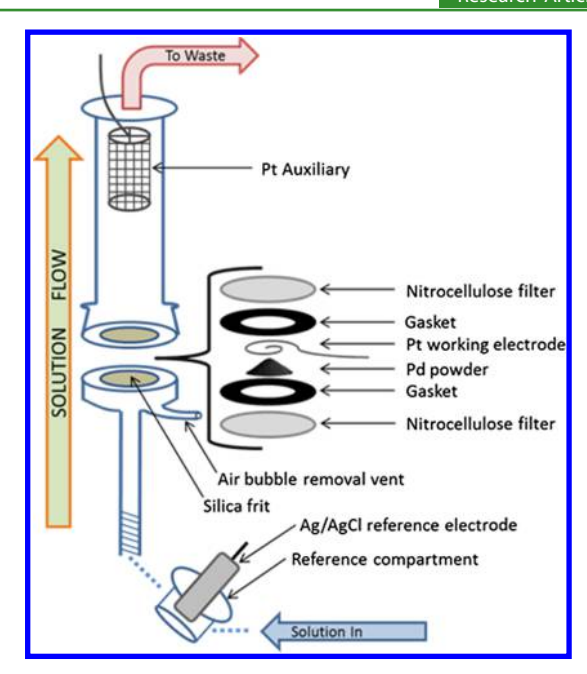


Figure 1. Powder flow cell.

cyclic voltammograms (CVs) were collected at a scan rate of 10 mV/s in 0.1 M  $\rm H_2SO_4.$ 

In each experiment, 50–300 mg of Pd powder (Sandia National Laboratories Powder Metallurgical Facility) was placed in the flow cell and soaked in 0.1 M  $\rm H_2SO_4$  for approximately 30 min to ensure uniform wetting of the membranes and the powder, promoting uniform solution flow and ensuring complete electrical connection. A voltammetric cleaning method similar to that used for planar  $\rm Au^{43}$  substrates was applied to clean the Pd powder, though the upper potential limit was decreased from 1.4 to 1.2 V to avoid oxygen evolution. After cycling the potential between -0.2 and +1.2 V in 0.1 M  $\rm H_2SO_4$  to clean the Pd surface, the potential cycling was stopped at 0.15 V and maintained before the experiment.

The procedure for Rh deposition using E-ALD is illustrated in Figure 2. A typical cycle involved flowing the Cu<sup>2+</sup> ion solution into the cell at a rate of 2 mL/min with the potential held at 0.15 V, until the solution was at equilibrium with the substrate, indicated by the absence of Cu deposition current. The potential was then allowed to go to open circuit, and the Rh solution was flowed through the cell. The Rh3+ solution was pumped through the cell until the potential increased to 0.39 V, a predetermined "stop" potential to avoid Pdoxidation. Reaching the stop potential is assumed to indicate that the Cu UPD atomic layer had been completely exchanged for 2/3 as many atoms of Rh, based on the expected stoichiometry. In the final step of the cycle, the Rh3+ solution was rinsed out with blank solution. Thicker Rh films were deposited by repeating this cycle the desired number of times on the Pd substrate. Deposits were performed where the Rh SLRR cycle was repeated 1, 3, 6, and 20 times on Pd powders. After deposition, the samples were rinsed with purified water and dried under vacuum.

Studies of the kinetics for hydrogen absorption and desorption were performed by modifying much smaller quantities of Pd powder, using a different flow cell configuration because of mass transport limitations that become important on fast timescales. This approach used a glassy carbon electrode, a GLAS-10 grade 1 cm<sup>2</sup> substrate (SPI Supplies), which had an exposed surface area of 0.71 cm<sup>32</sup>, defined by a Poly Donut masking tape (EPSI).

The studies of kinetics were performed in a standard E-ALD flow cell, with a few milligrams of Pd powder.<sup>44</sup> A 1 mg sample of Pd powder was studied by pressing it into the glassy C electrode surface before inserting it into the cell.<sup>44</sup> This sample was then placed in the flow cell on a 1.5 mm thick gasket (defining the solution volume) to perform electrochemical experiments.

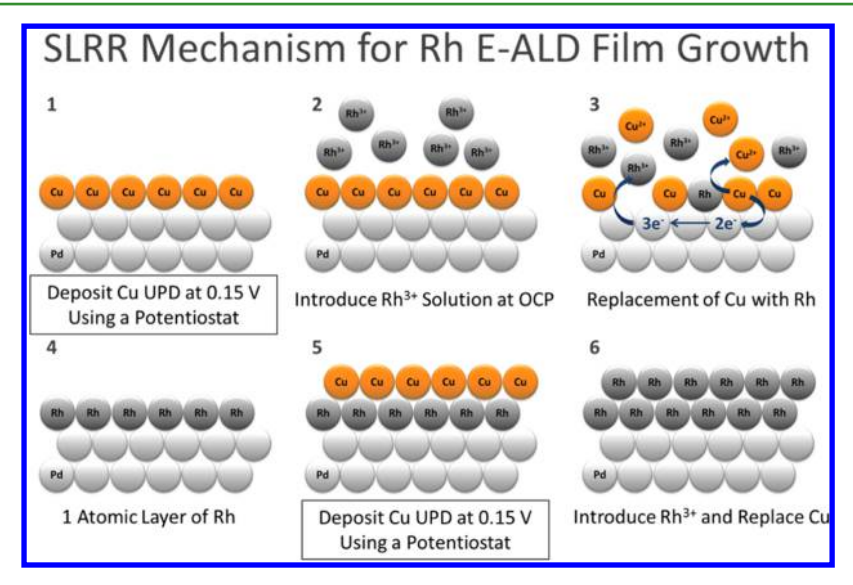


Figure 2. Rh deposition using SLRR.

Scanning electron microscopy (SEM) was performed using an FEI Inspect F system at 20 kV. X-ray photoelectron spectroscopy (XPS) data were obtained at the Advanced Light Source at Lawrence Berkeley National Laboratory (XPS endstation at beam line 9.3.2)<sup>45</sup> and by using a laboratory spectrometer with an Omicron DAR400 Al Kα X-ray source and a Physical Electronics 10-360 electron energy analyzer. Further details are available in the previously published work by Cappillino et al.40

The compositional distribution of Pd-Rh powder particles was imaged using scanning transmission electron microscopy (STEM). Following published literature, 46,47 the particles were mounted in epoxy (Struers) and then sectioned using a diamond knife on a Leica EM UC6 ultramicrotome. The resultant electron-transparent samples were subjected to compositional analysis using a probe-corrected FEI Titan G2 80-200 microscope with a large-area silicon drift energy dispersive X-ray spectroscopy (EDS) detector (Chemi-STEM). Individual EDS spectra were acquired at every image pixel for the EDS spectrum images. The Cliff–Lorimer k factor method was applied for the quantitative compositional analysis.  $^{48}$  The k factor was obtained from measurements of a known reference material (8 at % Rh-Pd), the composition of which was verified using X-ray fluorescence.

## 3. RESULTS

SEM images indicated that the particles were between 0.2 and  $0.4 \mu m$  (Figure 3). As expected, the Pd powder exhibited much higher currents than Pd films with an equivalent cross-section because of their greatly increased surface areas. Cyclic voltammetry was performed on 50 mg (black) and 300 mg samples of bare Pd powder (Figure 4, left). Starting at open

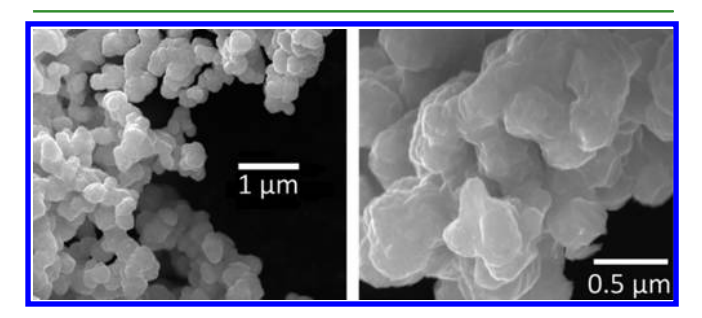


Figure 3. SEM images of unmodified Pd powder particles on two different scales.

circuit potential around 300 mV, the potential was scanned to -0.25 V. Hydrogen adsorption peaks begin just positive of 0 V, and the absorption peak begins at -0.1 V in the black plot for the 50 mg sample, but mostly overlaps with the adsorption peak in the red plot for the 300 mg sample. The scan was reversed at -0.25 V. Hydrogen desorption was evidenced by the rapid increase in current, which then decays and nears 0 mA around 0.1 V. Pd-oxidation features are seen during the positive scan starting at about 0.35 V and continuing until the scan was reversed at 1.2 V. The surface areas were measured by integration of the Pd oxide reduction peak<sup>49</sup> at 400 mV and found to be proportional to the mass of the powder (Figure 4, right). This suggests that the surface areas were equally accessed by solution. Comparing the charges for oxide reduction of SLRR Pd on Au and of powder samples to a physical vapor deposition (PVD) Pd film on a Si wafer allowed an estimate of the surface area per unit mass of powder, which is 0.4 m<sup>2</sup>/g (Table 1). The expected surface area for uniform spherical particles that do not touch is given by  $6/(\rho d)$ , where  $\rho$ is the density of the material and d is the particle diameter. Using the density of bulk Pd of about 12 g/cm<sup>3</sup>, this yields a particle diameter of slightly over 1  $\mu$ m. The actual particles in Figure 3 appear smaller but more occluded by interparticle contact and fusion; hence, the electrochemical measurement is reasonably consistent with the SEM observations.

Potential and current-time traces for Cu deposition on Pd powder for Rh exchange are shown in Figure 5. For this 300 mg Pd powder sample, a maximum of approximately 20 mA of current is observed. The time required to completely deposit the Cu was about 2 min, as indicated by the current returning to zero. The observed charge for the deposition was consistent with the measured surface area.

3.1. Cyclic Voltammetry of the Coated Samples. Cyclic voltammetry was performed on Pd powder samples coated with Rh, using the powder flow cell (Figure 1), to compare with uncoated Pd powder (Figure 6). The loss of Pd surface hydride peak area around 0 V indicates that Rh covers the Pd surface, preventing H adsorption. No kinetic enhancements in the rate of hydrogen absorption or desorption were observed from the CVs. This can be concluded because the CV profiles for proton reduction and hydrogen oxidation were essentially the same before and after the Rh SLRR cycles. Possibly, in both of these

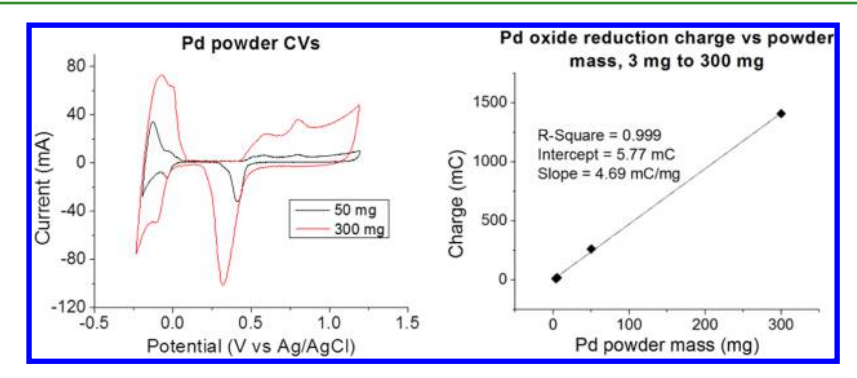
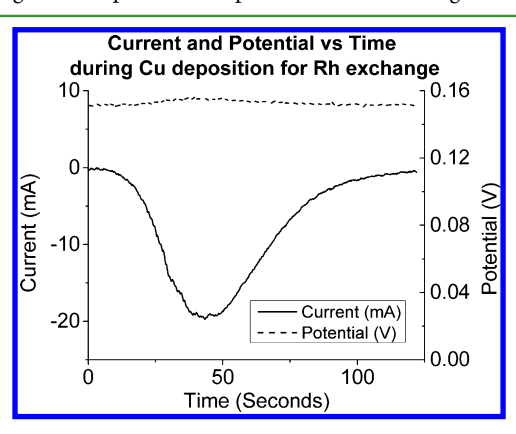


Figure 4. Pd powder CVs (left) and oxide reduction peak charges (right). The scan rate is 10 mV/s.

Table 1. Comparison of Pd Oxide Reduction Peak Charge and Calculated Surface Area for Various Samples<sup>a</sup>

Pd oxide reduction peak charge for surface area comparison versus Pd on Si		
sample	charge (mC)	normalized surface area (cm²)
Pd on Si wafer (2 cm <sup>2</sup> )	2.5	2
15 cycle Pd SLRR on Au film (2 cm²)	2.2	1.8
3.5 mg Pd powder	12	9.6
5 mg Pd powder	19.5	16
50 mg Pd powder	262	210
300 mg Pd powders	1410	1130

"Surface area is normalized against 2 cm<sup>2</sup> Pd on the Si wafer, by assuming that it represents complete Pd surface coverage.



**Figure 5.** Current (solid line) and potential (dashed line) during Cu deposition on the Pd powder.

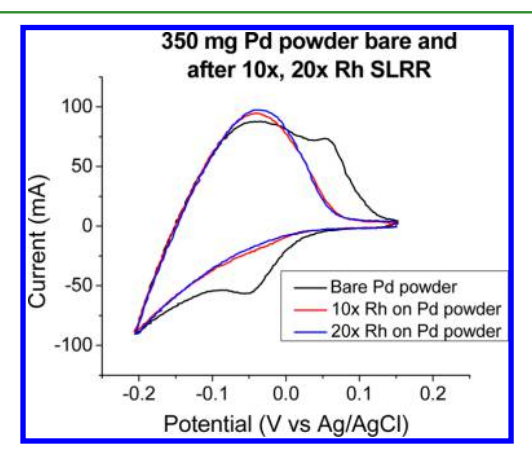


Figure 6. Overlaid CVs of 350 mg bare Pd (black), then modified by 10 (red) and 20 (blue) cycles of Rh SLRR.

CVs, current is limited by mass transport effects and solution resistance rather than the surface kinetics. CVs using smaller quantities of powder can be expected to allow more rapid transport into the interior of a powder mass and might yield observable kinetic effects, such as those previously shown; <sup>40</sup> hence, we have performed these experiments.

CVs of a powdered sample pressed into glassy carbon were run both before and after three Rh SLRR cycles (Figure 7). As

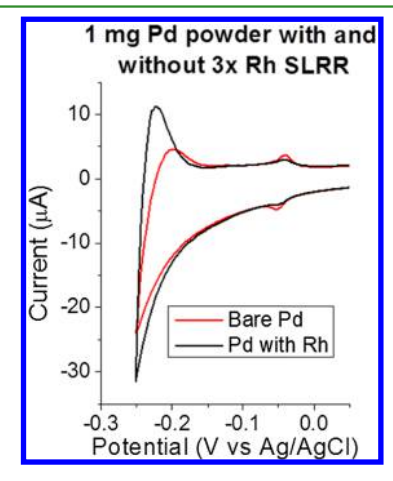


Figure 7. CV of the Pd powder bare (red) and modified by three cycles of Rh SLRR (black). The scan rate is 10 mV/s.

with Rh deposition on Pd films, the Pd surface hydride peaks at -0.05 V were diminished, indicating partial coverage of the surface by Rh, whereas the H absorption and desorption peaks showed higher currents that occurred earlier in the potential cycle. This demonstrates that, on a 1 mg sample, H sorption was faster when the surface was modified with Rh.

**3.2. STEM with EDS.** Figure 8 (middle) shows an overlay map of Rh and Pd STEM-EDS signals for epoxy-embedded, microtomed Pd powder samples on which one and six SLRR cycles for Rh had been performed. In both cases, there is an elevated Rh signal that follows the contour of the surface of the particle, including concave regions. The thickness was uniform to within a few nanometers in each case. Large bare regions with no Rh are not observed here. It is apparent that the Rh was not depositing as isolated islands on the length scale of these particles but was instead forming a uniform layer to within the resolution of the instrument, which approaches atomic dimensions. The quantity of Rh at the interface for the 6-cycle case is higher than the 1-cycle case but not by a factor of 6.

**ACS Applied Materials & Interfaces** 

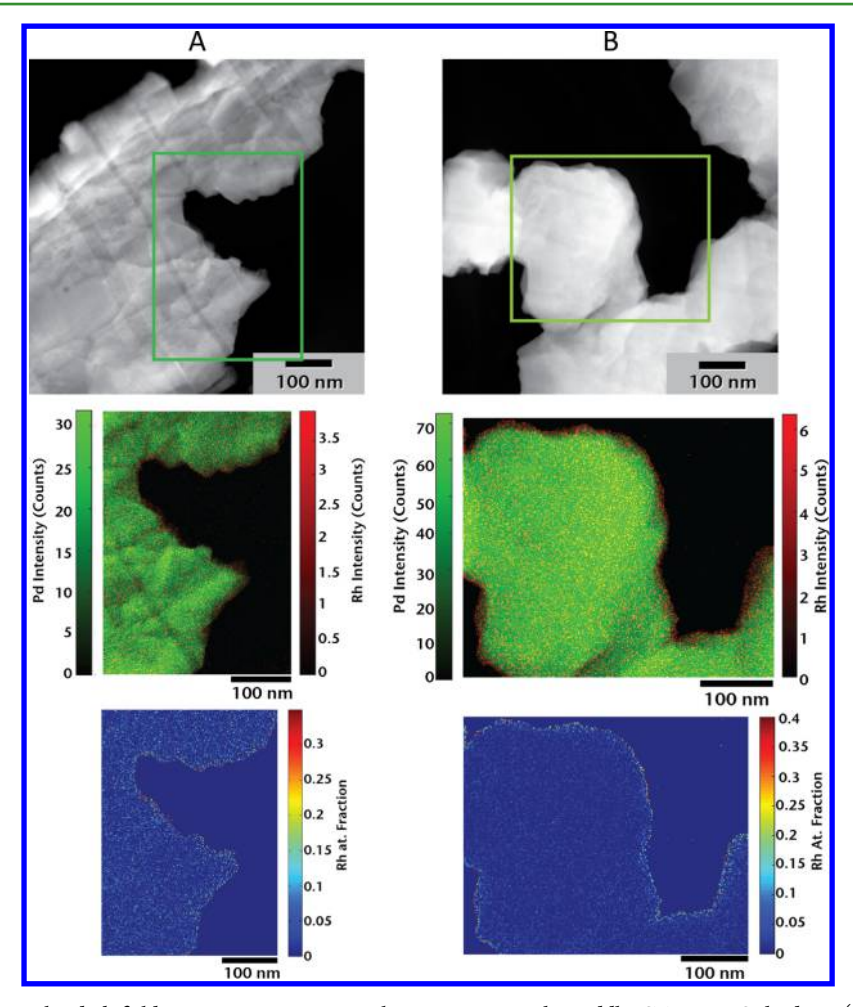


Figure 8. Top, high-angle annular dark field scanning transmission electron micrograph; middle, STEM-EDS rhodium (red) and palladium (green) overlay map; and bottom, Rh atomic fraction map of (A) 1-cycle Rh on Pd and (B) 6-cycle Rh on Pd.

**3.3. XPS.** XPS is complementary to STEM-EDS because it provides surface-specific information from a much larger volume of the sample. Lower incident photon energies have lower escape depths; hence, measuring the spectra at several photon energies provides greater detail concerning the surface structure than measurement at a single photon energy. Pd powder samples on which one, three, and six Rh cycles had been performed were measured using 450 and 850 eV synchrotron photons and using 1487 eV photons obtained on a laboratory instrument. The NIST software package SESSA was used to compute the simulated spectra for a bare Pd film, an 8 nm Rh film (essentially an infinitely thick Rh sample), and a 0.24 nm Rh layer on Pd, representing approximately one atomic layer.<sup>50</sup> Linear combinations of those spectra were compared with the experimental data to determine the best fit. The experimental and simulated spectra were backgroundcorrected and integrated in CasaXPS software using the Shirley method.51

Figure 9 displays the experimental and best-fit simulated data for one, three, and six cycles of Rh deposited on Pd. The amount of Rh increased with the number of cycles for both the simulations and experiments. The differences between the 450 eV spectra and those at higher incident energy were larger than the differences between 850 and 1487 eV, especially for the thicker films. This is due to the significantly lower electron escape depth for the 450 eV spectra.

The simulations (Figure 10) suggest that the one-cycle sample surface consisted of a mix of about 80% bare Pd and 20% thin Rh, and the three-cycle sample showed only a slightly thinner Rh. For comparison, the gas-phase ALD of Pd on alumina was reported to produce only about 20% coverage after 200 cycles.<sup>52</sup> The six-cycle sample, however, showed a significantly larger fraction of Rh and required ~2% coverage of thick Rh to obtain a best fit. Although the STEM-EDS images suggest that the layers are uniform and conformal on the scale of tens of nanometers, the XPS analysis suggests that some nonuniformity is present on different length scales. The average Rh thickness is primarily in the submonolayer regime for the few cycles performed in this study. If much threedimensional growth had been occurring, the fits to the XPS experiments would have appeared more like that of the 8.0 nm Rh simulation, and we would expect to see larger islands or dendrites in the STEM images. The simulated amounts of bare Pd are qualitatively consistent with the results from cyclic voltammetry, which showed a decreasing Pd surface hydride peak with increasing thickness, though some Pd surface hydride still formed after three cycles of Rh deposition.

# 4. CONCLUSIONS AND OUTLOOK

The use of E-ALD to grow nanofilms on a powdered electrode has been demonstrated. The rates of hydrogen absorption and desorption using Pd powder increased after monolayer-scale amounts of Rh were deposited, as observed using cyclic **ACS Applied Materials & Interfaces** 

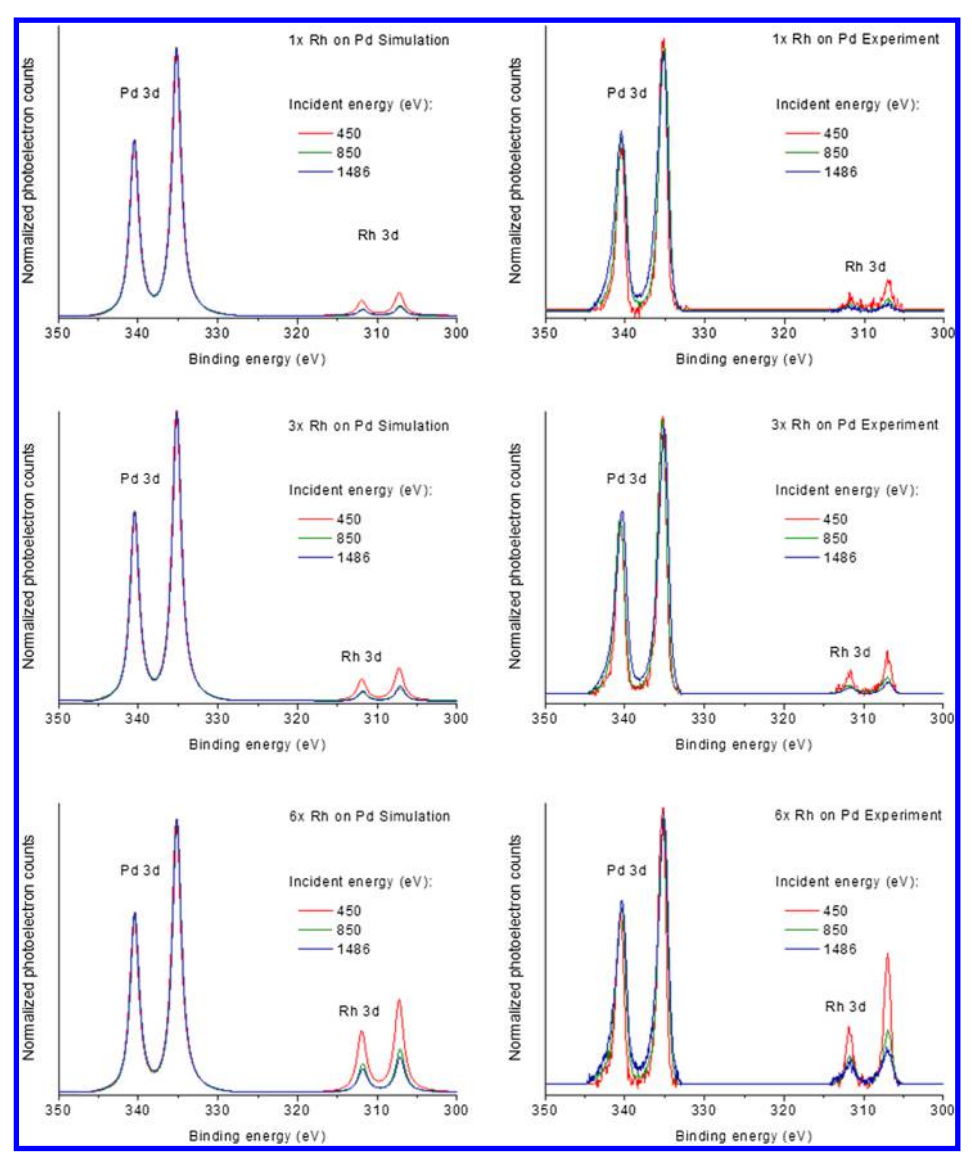
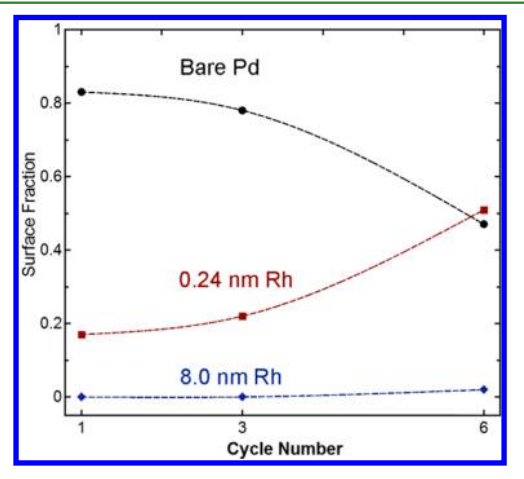


Figure 9. Experimental and simulated spectra at 450, 850, and 1486 eV for, top to bottom, one, three, and six cycles of Rh deposited on Pd powder. All spectra were background-subtracted and normalized to the area of the Pd peaks.



**Figure 10.** Contributions of each component to the best-fit simulation for each sample.

voltammetry. The voltammetry also indicated the presence of Rh on the surface through a decrease in the Pd surface hydride peaks. XPS analysis showed evidence of monolayer-scale Rh present on the surface, which increased with the number of cycles. STEM-EDS elemental mapping showed Rh confined to the outer surface of the Pd particles in a uniform, conformal coating on the nanometer length scale. The enhanced H absorption and desorption kinetics support the hypothesis that surface hydride is an intermediate state during bulk absorption and desorption. The presence of Rh appears to affect that intermediate state, possibly by destabilizing the surface hydride, reducing the activation barrier to transport out of the surface hydride state, and increasing the number of vacant surface hydride states.

This report suggests that the broad range of cycle chemistries accessible to the E-ALD method  $^{53,54}$  are applicable to powdered conductive substrates. The scale-up to larger quantities of powder may require a larger flow cell and counter electrode, and a potentiostat that can deliver adequate current. The presented experiments produced approximately  $50~\mu\rm A$  of current per mg of powder during Cu deposition, and the current can be expected to scale with the mass of the batch, assuming constant particle size, although mass transport

limitations and solution resistance may result in lower currents and longer cycle times. Agitation of the powder is a potential improvement of the process, which could enhance mass transport rates and increase the accessible surface area by breaking contact points between the particles. A similar and potentially more scalable deposition method, atomic layer electroless deposition (ALED), has been recently developed.<sup>40</sup> ALED applies a method similar to SLRR, except it uses hydrogen adsorbed or dilutely absorbed at the open circuit to act as a sacrificial element to allow a metal such as Rh to exchange and form a deposit on the metal surface.<sup>55</sup> Although ALED is less likely to suffer from the scaling limitations mentioned above, its versatility is limited by the number of substrates that can form surface hydrides. E-ALD has been demonstrated to form deposits in other potential ranges, not only where hydrides form. This work has helped establish that E-ALD is versatile not only in the materials that can be deposited but also in the substrates that can be used.

#### AUTHOR INFORMATION

### **Corresponding Author**

\*E-mail: stickney@uga.edu.

ORCID ®

David M. Benson: 0000-0002-3858-3382

The authors declare no competing financial interest.

#### ACKNOWLEDGMENTS

We acknowledge the support of the National Science Foundation, Division of Materials Research #1410109, and the Laboratory-Directed Research and Development program at Sandia National Laboratories, a multi-mission laboratory managed and operated by National Technology and Engineering Solutions of Sandia, LLC., a wholly owned subsidiary of Honeywell International, Inc., for the U.S. Department of Energy's National Nuclear Security Administration under contract DE-NA0003525. XPS data were obtained at the Advanced Light Source at Lawrence Berkeley National Laboratory (XPS endstation at beam line 9.3.2; Zhi Liu, beamline scientist) and supported by the Director, Office of Science, Office of Basic Energy Sciences, U.S. Department of Energy under contract no. DE-AC02-05CH11231.

#### REFERENCES

- (1) George, S. M. Atomic Layer Deposition: An Overview. Chem. Rev. 2010, 110, 111-131.
- (2) Christensen, S. T.; Feng, H.; Libera, J. L.; Guo, N.; Miller, J. T.; Stair, P. C.; Elam, J. W. Supported Ru-Pt Bimetallic Nanoparticle Catalysts Prepared by Atomic Layer Deposition. Nano Lett. 2010, 10, 3047-3051.
- (3) Lu, J.; Low, K.-B.; Lei, Y.; Libera, J. A.; Nicholls, A.; Stair, P. C.; Elam, J. W. Toward Atomically-Precise Synthesis of Supported Bimetallic Nanoparticles Using Atomic Layer Deposition. Nat. Commun. 2014, 5, 3264.
- (4) Adzic, R. R. Electrocatalytic Properties of the Surfaces Modified by Foreign Metal Adatoms; Wiley-Interscience: New York, 1984.
- (5) Kolb, D. M. Advances in Electrochemistry and Electrochemical Engineering; John Wiley: New York, 1978.
- (6) Magnussen, O. M. Ordered Anion Adlayers on Metal Electrode Surfaces. Chem. Rev. 2002, 102, 679-726.
- (7) Gregory, B. W.; Norton, M. L.; Stickney, J. L. Thin-Layer Electrochemical Studies of the Underpotential Deposition of Cadmium and Tellurium on Polycrystalline Au, Pt and Cu Electrodes. J. Electroanal. Chem. 1990, 293, 85-101.

- (8) Gregory, B. W.; Stickney, J. L. Electrochemical Atomic Layer Epitaxy (ECALE). J. Electroanal. Chem. Interfacial Electrochem. 1991, 300, 543-561.
- (9) Gregory, B. W.; Suggs, D. W.; Stickney, J. L. Conditions for the Deposition of CdTe by Electrochemical Atomic Layer Epitaxy. J. Electrochem. Soc. 1991, 138, 1279-1284.
- (10) Herrero, E.; Buller, L. J.; Abruña, H. D. Underpotential Deposition at Single Crystal Surfaces of Au, Pt, Ag and Other Materials. Chem. Rev. 2001, 101, 1897-1930.
- (11) Brankovic, S. R.; Wang, J. X.; Adžić, R. R. Metal Monolayer Deposition by Replacement of Metal Adlayers on Electrode Surfaces. Surf. Sci. 2001, 474, L173-L179.
- (12) Mrozek, M. F.; Xie, Y.; Weaver, M. J. Surface-Enhanced Raman Scattering on Uniform Platinum-Group Overlayers: Preparation by Redox Replacement of Underpotential-Deposited Metals on Gold. Anal. Chem. 2001, 73, 5953-5960.
- (13) Kim, Y.-G.; Kim, J. Y.; Vairavapandian, D.; Stickney, J. L. Platinum Nanofilm Formation by EC-ALE via Redox Replacement of UPD Copper: Studies Using In-Situ Scanning Tunneling Microscopy. J. Phys. Chem. B 2006, 110, 17998-18006.
- (14) Vasilic, R.; Dimitrov, N. Epitaxial Growth by Monolayer-Restricted Galvanic Displacement. Electrochem. Solid-State Lett. 2005,
- (15) Jayaraju, N.; Vairavapandian, D.; Kim, Y. G.; Banga, D.; Stickney, J. L. Electrochemical Atomic Layer Deposition (E-ALD) of Pt Nanofilms Using SLRR Cycles. J. Electrochem. Soc. 2012, 159,
- (16) Sheridan, L. B.; Gebregziabiher, D. K.; Stickney, J. L.; Robinson, D. B. Formation of Palladium Nanofilms Using Electrochemical Atomic Layer Deposition (E-ALD) with Chloride Complexation. Langmuir 2013, 29, 1592-1600.
- (17) Thambidurai, C.; Kim, Y.-G.; Stickney, J. L. Electrodeposition of Ru by Atomic Layer Deposition (ALD). Electrochim. Acta 2008, 53, 6157-6164.
- (18) Loukrakpam, R.; Yuan, Q.; Petkov, V.; Gan, L.; Rudi, S.; Yang, R.; Huang, Y.; Brankovic, S. R.; Strasser, P. Efficient C-C Bond Splitting on Pt Monolayer and Sub-Monolayer Catalysts During Ethanol Electro-Oxidation: Pt Layer Strain and Morphology Effects. Phys. Chem. Chem. Phys. 2014, 16, 18866-18876.
- (19) Sheridan, L. B.; Yates, V. M.; Benson, D. M.; Stickney, J. L.; Robinson, D. B. Hydrogen Sorption Properties of Bare and Rh-Modified Pd Nanofilms Grown via Surface Limited Redox Replacement Reactions. Electrochim. Acta 2014, 128, 400-405.
- (20) Jagannathan, K.; Benson, D. M.; Robinson, D. B.; Stickney, J. L. Hydrogen Sorption Kinetics on Bare and Platinum-Modified Palladium Nanofilms, Grown by Electrochemical Atomic Layer Deposition (E-ALD). J. Electrochem. Soc. 2016, 163, D3047-D3052.
- (21) Bartlett, P. N.; Marwan, J. The Effect of Surface Species on the Rate of H Sorption into Nanostructured Pd. Phys. Chem. Chem. Phys. 2004, 6, 2895-2898.
- (22) Greeley, J.; Mavrikakis, M. Surface and Subsurface Hydrogen: Adsorption Properties on Transition Metals and Near-Surface Alloys. J. Phys. Chem. B 2005, 109, 3460-3471.
- (23) Salloum, M.; James, S. C.; Robinson, D. B. Effects of Surface Thermodynamics on Hydrogen Isotope Exchange Kinetics in Palladium: Particle and Flow Models. Chem. Eng. Sci. 2015, 122,
- (24) Lin, S.; Shi, X.; Zhang, X.; Kou, H.; Wang, C. Ternary Semiconductor Compounds CuInS<sub>2</sub> (CIS) Thin Films Synthesized by Electrochemical Atomic Layer Deposition (EC-ALD). Appl. Surf. Sci. 2010, 256, 4365-4369.
- (25) Innocenti, M.; Becucci, L.; Bencistà, I.; Carretti, E.; Cinotti, S.; Dei, L.; Di Benedetto, F.; Lavacchi, A.; Marinelli, F.; Salvietti, E.; Vizza, F.; Foresti, M. L. Electrochemical Growth of Cu-Zn Sulfides. J. Electroanal. Chem. 2013, 710, 17-21.
- (26) Valdes, M.; Modibedi, M.; Mathe, M.; Hillie, T.; Vazquez, M. Electrodeposited Cu<sub>2</sub>ZnSnS<sub>4</sub> Thin Films. Electrochim. Acta 2014, 128, 393-399.

- (27) Zhang, L.; He, W.; Chen, X.-y.; Du, Y.; Zhang, X.; Shen, Y.; Yang, F. Nanocrystallized Cu<sub>2</sub>Se Grown on Electroless Cu Coated P-Type Si Using Electrochemical Atomic Layer Deposition. *Surf. Sci.* **2015**, *631*, 173–177.
- (28) Brankovic, S. R.; Wang, J. X.; Adžić, R. R. Pt Submonolayers on Ru Nanoparticles: A Novel Low Pt Loading, High CO Tolerance Fuel Cell Electrocatalyst. *Electrochem. Solid-State Lett.* **2001**, *4*, A217—A220.
- (29) Li, M.; Yang, W. F. Highly Porous Palladium Bulk: Preparation and Properties as Active Metal Material for Displacement Chromatographic Process. *Int. J. Hydrogen Energy* **2009**, *34*, 1585–1589.
- (30) Antolini, E. Palladium in Fuel Cell Catalysis. *Energy Environ. Sci.* **2009**, *2*, 915–931.
- (31) Leparmentier, S.; Auguste, J.-L.; Humbert, G.; Delaizir, G.; Delepine-Lesoille, S.; Bertrand, J.; Buschaert, S.; Perisse, J.; Macé, J. R. Palladium Particles Embedded into Silica Optical Fibers for Hydrogen Gas Detection. *Proc. SPIE* **2014**, *9128*, 91280H.
- (32) Shao, M. Palladium-Based Electrocatalysts for Hydrogen Oxidation and Oxygen Reduction Reactions. *J. Power Sources* **2011**, 196, 2433–2444.
- (33) Kibria, A. K. M. F.; Sakamoto, Y. The Effect of Alloying of Palladium with Silver and Rhodium on the Hydrogen Solubility, Miscibility Gap and Hysteresis. *Int. J. Hydrogen Energy* **2000**, *25*, 853–859.
- (34) Lototsky, M. V.; Williams, M.; Yartys, V. A.; Klochko, Y. V.; Linkov, V. M. Surface-Modified Advanced Hydrogen Storage Alloys for Hydrogen Separation and Purification. *J. Alloys Compd.* **2011**, 509, S555–S561.
- (35) Mallát, T.; Polyánszky, É.; Petró, J. Electrochemical Study of Palladium Powder Catalysts. *J. Catal.* **1976**, *44*, 345–351.
- (36) Zhang, J.; Bai, Q.; Zhang, Z. Dealloying-Driven Nanoporous Palladium with Superior Electrochemical Actuation Performance. *Nanoscale* **2016**, *8*, 7287–7295.
- (37) Ward, T. L.; Dao, T. Model of Hydrogen Permeation Behavior in Palladium Membranes. *J. Membr. Sci.* **1999**, *153*, 211–231.
- (38) Foltz, G. W.; Melius, C. F. Studies of Isotopic Exchange Between Gaseous Hydrogen and Palladium Hydride Powder. *J. Catal.* **1987**, *108*, 409–425.
- (39) Heung, L. K.; Sessions, H. T.; Xiao, X. TCAP Hydrogen Isotope Separation Using Palladium and Inverse Columns. *Fusion Sci. Technol.* **2011**, *60*, 1331–1334.
- (40) Cappillino, P. J.; Sugar, J. D.; El Gabaly, F.; Cai, T. Y.; Liu, Z.; Stickney, J. L.; Robinson, D. B. Atomic-Layer Electroless Deposition: A Scalable Approach to Surface-Modified Metal Powders. *Langmuir* **2014**, *30*, 4820–4829.
- (41) Łukaszewski, M.; Hubkowska, K.; Czerwiński, A. Electrochemical Absorption and Oxidation of Hydrogen on Palladium Alloys with Platinum, Gold and Rhodium. *Phys. Chem. Chem. Phys.* **2010**, *12*, 14567–14572.
- (42) Żurowski, A.; Łukaszewski, M.; Czerwiński, A. Electrosorption of Hydrogen into Palladium—Rhodium Alloys. *Electrochim. Acta* **2006**, *51*, 3112—3117.
- (43) Sheridan, L. B.; Czerniawski, J.; Jayaraju, N.; Gebregziabiher, D. K.; Stickney, J. L.; Robinson, D. B.; Soriaga, M. P. Electrochemical Atomic Layer Deposition (E-ALD) of Palladium Nanofilms by Surface Limited Redox Replacement (SLRR), with EDTA Complexation. *Electrocatalysis* **2012**, *3*, 96–107.
- (44) Flowers, B. H., Jr.; Wade, T. L.; Garvey, J. W.; Lay, M.; Happek, U.; Stickney, J. L. Atomic Layer Epitaxy of CdTe Using an Automated Electrochemical Thin-Layer Flow Deposition Reactor. *J. Electroanal. Chem.* 2002, 524–525, 273–285.
- (45) Grass, M. E.; Karlsson, P. G.; Aksoy, F.; Lundqvist, M.; Wannberg, B.; Mun, B. S.; Hussain, Z.; Liu, Z. New Ambient Pressure Photoemission Endstation at Advanced Light Source Beamline 9.3.2. *Rev. Sci. Instrum.* **2010**, *81*, 053106.
- (46) Johnson, P. B.; Thomson, R. W.; Reader, K. TEM and SEM Studies of Radiation Blistering in Helium-Implanted Copper. *J. Nucl. Mater.* **1999**, 273, 117–129.
- (47) Hochella, M. F., Jr.; Moore, J. N.; Golla, U.; Putnis, A. A TEM Study of Samples from Acid Mine Drainage Systems: Metal-Mineral

- Association with Implications for Transport. *Geochim. Cosmochim. Acta* **1999**, *63*, 3395–3406.
- (48) Cliff, G.; Lorimer, G. W. The Quantitative Analysis of Thin Specimens. J. Microsc. 1975, 103, 203–207.
- (49) Rand, D. A. J.; Woods, R. A Study of the Dissolution of Platinum, Palladium, Rhodium and Gold Electrodes in 1 M Sulphuric Acid by Cyclic Voltammetry. J. Electroanal. Chem. Interfacial Electrochem. 1972, 35, 209–218.
- (50) Smekal, W.; Werner, W. S. M.; Powell, C. J. Simulation of Electron Spectra for Surface Analysis (SESSA): A Novel Software Tool for Quantitative Auger-Electron Spectroscopy and X-ray Photoelectron Spectroscopy. Surf. Interface Anal. 2005, 37, 1059–1067.
- (51) Fairley, N. CasaXPS Manual 2.3.15; Acolyte Science, 2009.
- (52) Weber, M. J.; Mackus, A. J. M.; Verheijen, M. A.; Longo, V.; Bol, A. A.; Kessels, W. M. M. Atomic Layer Deposition of High-Purity Palladium Films from  $Pd(hfac)_2$  and  $H_2$  and  $O_2$  Plasmas. *J. Phys. Chem. C* **2014**, *118*, 8702–8711.
- (53) Stickney, J. L. Electrochemical Atomic Layer Epitaxy; Rubinstein, I., Bard, A. J., Eds.; Marcel Dekker: New York, 1999; pp 75–209.
- (54) Switzer, J. A. Atomic Layer Electrodeposition. *Science* **2012**, 338, 1300–1301.
- (55) Nutariya, J.; Fayette, M.; Dimitrov, N.; Vasiljevic, N. Growth of Pt by Surface Limited Redox Replacement of Underpotentially Deposited Hydrogen. *Electrochim. Acta* **2013**, *112*, 813–823.